Elsevier required licence: © <2020>. This manuscript version is made available under the CC-BY-NC-ND 4.0 license http://creativecommons.org/licenses/by-nc-nd/4.0/
The definitive publisher version is available online at
[https://www.sciencedirect.com/science/article/pii/S0040609020305125]

ResearchGate

See discussions, stats, and author profiles for this publication at: https://www.researchgate.net/publication/343811482

Electrical and optical properties in O-polar and Zn-polar ZnO films grown by pulsed laser deposition

Article *in* Thin Solid Films · August 2020

DOI: 10.1016/j.tsf.2020.138303

CITATIONS
0

READS
25

7 authors, including:

Md. Azizar Rahman
University of Technology Sydney
30 PUBLICATIONS **218** CITATIONS

SEE PROFILE

Maik Butterling
Delft University of Technology
50 PUBLICATIONS **330** CITATIONS

SEE PROFILE

Andreas Wagner
Helmholtz-Zentrum Dresden-Rossendorf
370 PUBLICATIONS **5,663** CITATIONS

SEE PROFILE

Some of the authors of this publication are also working on these related projects:

Heavy ion physics View project

radiation effects View project

All content following this page was uploaded by Chi-Chung Ling on 24 August 2020.

The user has requested enhancement of the downloaded file.

Journal Pre-proof

Electrical and optical properties in O-polar and Zn-polar ZnO films grown by pulsed laser deposition

Caiqin Luo , M. Azizar Rahman , Matthew R. Phillips , Cuong Ton-That , M. Butterling , A. Wagner , Francis Chi-Chung Ling

PII: S0040-6090(20)30512-5
DOI: https://doi.org/10.1016/j.tsf.2020.138303
Reference: TSF 138303

To appear in: *Thin Solid Films*

Received date: 13 February 2020
Revised date: 19 August 2020
Accepted date: 21 August 2020

Please cite this article as: Caiqin Luo , M. Azizar Rahman , Matthew R. Phillips , Cuong Ton-That , M. Butterling , A. Wagner , Francis Chi-Chung Ling , Electrical and optical properties in O-polar and Zn-polar ZnO films grown by pulsed laser deposition, *Thin Solid Films* (2020), doi: https://doi.org/10.1016/j.tsf.2020.138303

This is a PDF file of an article that has undergone enhancements after acceptance, such as the addition of a cover page and metadata, and formatting for readability, but it is not yet the definitive version of record. This version will undergo additional copyediting, typesetting and review before it is published in its final form, but we are providing this version to give early visibility of the article. Please note that, during the production process, errors may be discovered which could affect the content, and all legal disclaimers that apply to the journal pertain.

© 2020 Published by Elsevier B.V.

Journal Pre-proof

HIGHLIGHTS

- Zn- and O-polar ZnO films grown by pulsed laser deposition were characterized.
- Their electrical and optical properties are dependent on the polarity.
- The differences in the properties are explained by the presence of different defects.

Journal Pre-proof

Electrical and optical properties in O-polar and Zn-polar ZnO films grown by pulsed laser deposition

Caiqin Luo[1,⁋], M. Azizar Rahman[2,‡], Matthew R. Phillips[2], Cuong Ton-That[2], M. Butterling[3], A. Wagner[3], Francis Chi-Chung Ling[1,*]

[1] *Department of Physics, The University of Hong Kong, Pokfulam Road, Hong Kong, China*

[2] *School of Mathematical and Physical Sciences, University of Technology Sydney, Ultimo, NSW, 2007, Australia*

[3] *Institute of Radiation Physics, Helmholtz-Zentrum Dresden-Rossendorf, Bautzner Landstr., 400, 01328m Dresden, Germany*

[*] Corresponding Author: ccling@hku.hk

[⁋] Present address: Henan Key Laboratory of Photovoltaic Materials, Henan University, Kaifeng, China

[‡] Present address: Bangladesh University of Engineering and Technology, Dhaka 1000, Bangladesh

O-polar and Zn-polar ZnO films were grown on c-sapphire by pulsed laser deposition. Positron annihilation spectroscopy study reveals that the V_{Zn}-related defects in the ZnO films with different polarities are different in structure and their thermal evolution is different. Hall effect measurement and luminescence spectroscopy reveal that the electrical and optical properties and their corresponding thermal evolution are strongly dependent on the polarity of the film. The luminescence spectra of the as-grown Zn-polar ZnO film is signified by a negligible green defect emission (at ~ 2.4 eV) and strong near band edge emission as compared with the O-polar film. The as-grown Zn-polar film exhibited a lower electron concentration (2×10^{18} cm^{-3}) than that of the O-polar film (6×10^{18} cm^{-3}); this difference is attributed to their different H concentrations. For the O-polar film, the electron concentration decreased with annealing temperature T_{anneal}, reaching a minimum at 700°C and then increased to 4×10^{18} cm^{-3} at T_{anneal} = 900 °C. In comparison, the electron concentration of the Zn-polar ZnO film monotonically decreased with T_{anneal} attaining a value of ~1×10^{17} cm^{-3} at T_{anneal} = 900 °C, 40 times smaller than that of the O-polar film. The cause for the differences

in the optical and electrical properties for the O-polar and Zn-polar films is explained by the presence of different defects in these films.

KEYWORDS: Zinc oxide; Polarity; Pulsed laser deposition; Magnesium oxide; Buffer layer; Luminescence spectroscopy; Positron annihilation spectroscopy; Hall effect measurement; Annealing

Journal Pre-proof

Introduction

ZnO, a wide band gap semiconductor, has received extensive attention because of its wide range of technological applications, including optoelectronics, spintronics, transparent electrodes, sensor devices, and photocatalysis [1]. However, the asymmetric p-type doping challenge remains as a significant obstacle to the development of reliable ZnO-based device technology. The realization of p conductivity is particularly difficult because of (i) the high ionization energies of the traditional acceptors, (ii) the low solubility of p-dopants and (iii) strong self-compensation by native defects. Recent studies suggest that a potential shallow acceptor in ZnO could be a complex involving a substitutional dopant , for example the V_{Zn}-N_O shallow acceptor in N-doped ZnO [2, 3], whose formation is favored by Zn-polar growth [2]. Significantly, it has been reported that group V elements P, As and Sb on Zn cation sites can produce a shallow acceptor through the creation of a defect complex with two zinc vacancies, X_{Zn}-$2V_{Zn}$,(X=P, As or Sb) [4]. In support of this model, Hsu et al. [5] observed p-type conductivity in hydrothermally grown undoped ZnO nanorods and found that the p-type conductivity was directly correlated with the number of V_{Zn}-related defects. . Furthermore, in Al or Ga-doped ZnO transparent electrodes, the formation of the Al_{Zn}-V_{Zn} (or Ga_{zn}-V_{zn}) compensating acceptors, enhanced by n^+-doping, limits the resultant electron concentration and the performance of the n^+ material [6, 7]. These results indicate that understanding the properties of V_{Zn}-related defects in the ZnO films and measuring their abundance is crucial to progress research to achieve reliable p-type conductivity in ZnO. However, despite their importance, many of the fundamental properties of intrinsic V_O and V_{Zn} in ZnO remain controversial. The V_{Zn} in ZnO is a two-level deep acceptor [8, 9] , which has a low formation energy. Using positron annihilation spectroscopy (PAS), Saarinen et al. [10] showed that V_{Zn} were the prevalent residual acceptors in undoped ZnO single crystals. For pulsed laser deposition (PLD) grown undoped ZnO film grown on c-sapphire, it was found that the

Journal Pre-proof

vacancy cluster V_{Zn}-$2V_O$ was the only identified dominant V_{Zn}-related defect [11]. The authors suggested that vacancy cluster is favored over isolated V_{Zn} despite of the relatively high formation energy of the vacancy cluster because of the high dissociation energy of the vacancy cluster and the low substrate temperature (600 ^oC). This implied that the vacancy cluster once formed was not easily thermally dissociated and thus its formation was governed by diffusion kinetics rather than a thermodynamic process. It is commonly accepted that V_O is a negative-U deep donor being stable in either its neutral or doubly ionized state, although the formation energy obtained from the first principles calculation is reported to diverge [8, 9, 12]. A number of different broad green luminescence (GL) peaks in ZnO are attributed to both V_O and V_{Zn} defects ([8, 13] and references therein). However, a recent hybrid density functional study of ZnO in a one-dimensional configuration suggested that V_{Zn} are not responsible for the GL [14].

The wurtzite structure of ZnO lacks the center of symmetry, resulting in the spontaneous polarization of Zn-terminated (0001) surface and O-terminated ($000\bar{1}$) surface [15]. The Zn-polar and O-polar faces of ZnO exhibit distinct physical properties and consequently when used in device fabrication each face can provide different performance capabilities in light emitting diodes (LED), Schottky diodes, solar cells and photocatalytic activity (see [15] and references in [16]). Pulsed laser deposition (PLD) is a method commonly used to fabricate oxide films and has widely used in ZnO growth (like [17-20] and page 34 in the review [1]). For ZnO thin films, polarity control is usually achieved by the growth using the expensive and complicated methods molecular beam epitaxy and metalorganic vapour-phase epitaxy. Luo et al. [16] recently demonstrated the growth of Zn-polar and O-polar ZnO films on c-sapphire by PLD simply by varying the thickness of a MgO buffer layer. PLD growth has the advantages of its simple experimental setup,

Journal Pre-proof

relatively less costly, operation in high ambient gas pressures, low substrate temperature, and relatively good crystalline quality.

No systematic study on the electrical and optical property dependences on the polarity of ZnO films fabricated by PLD has been reported in the literature. In the present study, undoped Zn-polar and O-polar ZnO films were grown on c-sapphire by PLD and comprehensively characterized by Hall effect measurements, luminescence spectroscopy and secondary ion mass spectroscopy (SIMS). The V_{Zn}-related defects in the O-polar and Zn-polar ZnO samples were investigated by PAS. The effect of thermal annealing was also investigated.

Experimental

The undoped ZnO films were grown on c-plane sapphire by PLD. The polarity of the ZnO film was controlled using MgO buffer layer. The ZnO films grown without the MgO buffer are O-polar conversely those grown with a 5 nm MgO buffer layer are Zn-polar. [16]. A ZnO target having the purity of 99.999 % was used for the ablation sources. The ceramic target with diameter of 2 inch was obtained commercially from Kurt J. Lesker, U.S. The background pressure of the growth chamber was 10^{-4} Pa. A KrF excimer laser with the wavelength of 248 nm, pulse energy of 300 mJ and repetition frequency of 2 Hz was used to ablate the target. The target-substrate separation was 6.5 cm. The substrate temperature and the oxygen pressure was kept at 600 ^{o}C and 0.02 Pa respectively during the growth. These growth parameters yielded one of the samples having the narrowest full width half maximum (FWHM) of the (002) X-ray diffraction (XRD) peak. The film thickness was measured by the cross sectional scanning electron microscope (SEM) image and the film growth rates were ~1.7 nm/min and ~2.7 nm/min for the O-polar and Zn-polar films respectively [16]. Controlled by the growth time, the thicknesses of the films used in the present study were

Journal Pre-proof

kept at ~100 nm for the SIMS study and ~300 nm for the PAS, photoluminescence (PL), cathodoluminescence (CL) and Hall studies. The details of the fabrication and polarity characterization are given in reference [16]. The isochronal annealing was carried out in Ar atmosphere for a period of 45 minute. Room temperature Hall measurement was performed using the Accenet HL-5500PC system and the van der Pauw configuration. Time-of-flight Secondary Ion Mass (SIMS) Spectrometer (ION-TOF GmbH) was used to study the depth profile of the ZnO film sample. The instrument was equipped with a 25 keV Bi_1 cluster gun as the primary ion source and a 3 keV Cs+ ion source for etching. The primary ion beam (1 pA, 5.46×10^{14} Ions/cm^2) had a focus area approximately 49×49 μm^2. The Cs+ beam current, crater area and sputter ion density were 33 nA, 300×300 μm^2 and 4.74×10^{17} ions/cm^2 respectively. The 325 nm line from the Kimmon He-Cd laser was used as the excitation source for the PL study. The 500 nm focal length monochrometer (Omni-λ 508), the photomultiplier and the lock-in amplifier were used for the PL spectrum acquisition. The sample was loaded into the Oxford closed cycle He refrigerator for keeping the sample at the temperature of 10 K during the PL measurement. The CL measurements were performed at the temperature of 80 K using the FEI Quanta 200 scanning electron microscope (SEM) equipped with a parabolic mirror, an Oriel MS257 monochromator and a Hamatmatsu S7011-1077 CCD sensor. To obtain the depth profiling of the CL, electron beam energy was varied from 2 keV to 10 keV while keeping the excitation power constant at 30 μW. All luminescence data were corrected for the total response of the light collection system.

Coincidence Doppler broadening spectroscopy (CDBS) study, which is a kind of PAS, was performed using a continuous mono-energetic positron beam having a maximum positron energy of 35 keV. The annihilation gamma photon energy spectrum was collected by two high purity Ge detectors and the corresponding nuclear electronics having an energy resolution of 1.09 keV. The Doppler broadening of the annihilation gamma line at 511 keV

Journal Pre-proof

was monitored by the S-parameter defined as the count of the central window at 511± 0.76 keV divided by the total count of the 511 keV peak; and the W-parameter defined as the count of the two wing windows at 511-6.8 eV to 511-3.4 keV and 511+3.4 keV to 511+6.8 keV. Experimental details of the CDBS study can be found in reference [11].

Results

Two types of undoped ZnO samples were fabricated on c-sapphire by PLD, one with a Zn-polar face grown with a 5 nm MgO buffer layer and the other with a O-polar face grown without a buffer layer [16]. In the previous study [16], the surfaces of both the as-grown samples were chemically etched with nitric acid solution (0.02 M) and subsequently studied by SEM. The results indicated that chemical etching behavior is strongly dependent on the surface polarity of ZnO [21-23]. After etching, ZnO samples grown with and without the buffer layer exhibit a hexagonal pit pattern and hill rock pattern respectively, revealing the surface terminations of Zn and O polar faces [16]. XRD study was performed on the as-grown O-polar and Zn-polar undoped ZnO samples. Both the Zn- and O-polar samples exhibit a predominant (002) orientation as indicated by the XRD patterns of all the samples that show a strong ZnO (002) peak with (100), (101), (103) and (200) peaks that are at least 100 times weaker in intensity. [16].

Hall measurements revealed that the as-grown O-polar sample and the Zn-polar samples have different electron concentrations of 6×10^{18} cm^{-3} and 2×10^{18} cm^{-3}, respectively. Figure 1(a) shows the electron concentration of the undoped O-polar and Zn-polar ZnO samples versus the annealing temperature. For the O-polar undoped ZnO samples, the electron concentration slightly decreases to ~2×10^{18} cm^{-3} as the annealing temperature increases to 700 ^{o}C, and then increases with annealing temperature to ~4×10^{18} cm^{-3} as the annealing temperature reaches 900 ^{o}C. Whereas, the electron concentration of the Zn-polar

undoped ZnO samples has a completely different trend of thermal evolution. Conversely, it decreases monotonically with annealing temperature and reaches the value of 1×10^{17} cm^{-3} at 900 ^{o}C, which is 40 times smaller than the value of the O-polar sample.

The hydrogen SIMS depth profile of the as-grown O-polar ZnO sample as shown in the insert of Figure 1(b) reveals a uniform spatial distribution of hydrogen in the sample. Similar results were found for all the O-polar and Zn-polar undoped ZnO samples annealed at the different annealing temperatures. Figure 1(b) shows the relative hydrogen SIMS intensity against the annealing temperature for the O-polar and Zn-polar undoped ZnO samples. The as-grown undoped O-polar ZnO sample has ~3.7 times higher H concentration than that of the Zn-polar sample. The H concentration in the O-polar undoped sample dramatically drops by 69 % after annealing at 750 ^{o}C, followed by further slight drop of ~5 % after annealing at 900 ^{o}C. For the Zn-polar undoped ZnO sample, its H concentration slightly decreases with the annealing temperature, with only ~5 % drop after annealing at 750 ^{o}C and another 5 % after annealing at 900 ^{o}C.

A CDBS study was performed on the O-polar and Zn-polar undoped ZnO samples annealed at different temperatures up to 800 ^{o}C. CDBS is a specialized type of PAS which is selectively sensitive to V_{Zn}-related defects in ZnO [24]. The mean positron implantation depth is given by: $x = AE^{1.6}/\rho$, where ρ is the density and A=4.0 µgcm^{-2}keV$^{-1.6}$ is a constant [24]. A positron energy of 5 keV refers to the positron implantation depth of ~140 nm. As the film thickness is ~300 nm and the positron diffusion length is measured to be ≤30 nm for the current samples, nearly all the positrons implanted at 5 keV annihilate in the bulk film. Accordingly, the S and W parameters measured at 5 kV are representative of the bulk film.

Figure 2 shows the W-parameter against the S-parameter for the Zn-polar undoped ZnO samples grown with $P(O_2)$=0.02 Pa annealed at different temperatures (as-grown, 700 ^{o}C and 800 ^{o}C). We have performed a systematic CDBS study on the O-polar undoped ZnO

samples grown with different P(O_2) conditions (= 0 Pa, 0.02 Pa and 1.30 Pa) and annealed at different annealing temperatures (as-grown, 750 ^{o}C and 900 ^{o}C), and the corresponding (W,S) data are shown in Figure 2 [11]. These W- and S-parameters are normalized against those from a high quality ZnO single crystal which exhibited a single positron lifetime of 166 ps, confirming that the single crystal sample is close to defect free [11]. The (W,S) data of this single crystal sample is also plotted in Figure 2. As positrons implanted into the sample will be rapidly thermalized and undergo diffusion, if vacancy type defects exist the mobile positrons will be captured by the potential well of the missing atomic core of the vacancy. Positrons can then either finally annihilate with a surrounding electron either in the delocalized bulk state while in diffusion (state *b*), or in the localized defect states (states d_i). The measured S-parameter is the weighted sum of the contributions from the different positron states, i.e. $S = f_b S_b + f_{di} S_{di}$, where f_i and S_i are the fraction of annihilating at state i and the characteristic S-parameter of state I respectively. Similarly, the corresponding W-parameter is given by: $W = f_b W_b + f_d W_d$. If a single type of defect exists, then combining the two S and W expressions yields: $(S - S_b)/(W - W_b) = (S_d - S_b)/(W_d - W_b)$. This relationship shows that a straight line passing through the (W,S) data of the defect free sample will be yielded and its slope is the fingerprint of the corresponding vacancy type defect.

Makkonen et al. [25] carried out theoretical study on the Doppler broadening of the annihilation radiation from the V_{Zn} state and the vacancy clusters states in ZnO. The theoretical W-S straight lines (which are fingerprints of the vacancy type defects, as shown above) of the different V_{Zn}-related defects are included in Figure 2 for reference. It was found that the theoretical characteristic (W,S) values of V_{Zn}, V_{Zn}-V_O, $2V_{Zn}$-V_O and $4V_{Zn}$-V_O are not easily distinguishable by the CDBS. Adding a V_O and a V_{Zn} to the vacancy structure have the effect of shifting the (W,S) data to horizontally right (i.e. increase of S-parameter)

and vertically down respectively (decrease of W-parameter). The characteristic W-S line of the $4V_{Zn}$ is at the lower left side to that of V_{Zn}, V_{Zn}-V_O, $2V_{Zn}$-V_O and $4V_{Zn}$-V_O, while that of V_{Zn}-$2V_O$ is at the upper right side. The annealing behavior of the O-polar undoped ZnO samples are very similar and independent of the oxygen pressure $P(O_2)$ during growth. It can be seen from Figure 2, regardless of the growth $P(O_2)$, the (W,S) data of the as-grown and the 750 ^oC annealed O-polar ZnO samples lay on the theoretical characteristic W-S line of V_{Zn}-$2V_O$, and are thus associated with a V_O-rich tri-vacancy cluster. This implies that the V_{Zn}-$2V_O$ is the only V_{Zn}-related defect that exists in these samples. As the annealing temperature increases to 900 ^oC, the W-S data moves slightly away from the characteristic line though with a magnitude slightly larger than the experimental error, which is associated with the co-existence of V_{Zn}-$2V_O$ and new thermally induced V_{Zn}-related defect containing more V_{Zn} or less V_O.

For the as-grown undoped Zn-polar ZnO samples fabricated with 0.02 Pa for which its (W,S) data lays between the theoretical fingerprint lines, more than one type of V_{Zn}-related defect exists. The defect candidates in this case would include the V_{Zn}-$2V_O$ that is detected in the as-grown O-polar ZnO sample, and possibly V_{Zn}, V_{Zn}-V_O and $2V_{Zn}$-V_o defects that are not distinguishable by CDBS. After annealing at 900 ^oC, the (W,S) data lays on the theoretical characteristic W-S line of V_{Zn}, V_{Zn}-V_O and $2V_{Zn}$-$2V_O$ which is also indistinguishable by CDBS. This means that any of these three defects could exist on their own, or that they could co-exist together. However, it can be unambiguously concluded that after annealing at 900 ^oC that: (i) no V_{Zn}-$2V_O$ was detected in the Zn-polar sample; and (ii) in O-polar sample V_{Zn}-related defects containing relatively more V_{Zn} and less V_O is formed in addition to V_{Zn}-$2V_O$. These results collectively reveal that that the O-polar and Zn-polar ZnO materials contain different V_{Zn}-related defects and exhibit dissimilar thermal behaviors.

Journal Pre-proof

Figure 3(a) shows the low temperature (10 K) PL spectra for the as-grown O-face and Zn-face ZnO samples. The near band edge emission (NBE) at 3.351 eV, and two deep level emission (DLE) peaks namely the GL at 2.27 eV and the blue emission at 2.96 eV, are observed in the PL spectra of the O-face sample. In contrast, for the as-grown Zn-polar ZnO sample, the DLE intensity is negligible and the NBE intensity is 20 times stronger than that of the O-polar sample. The GL without fine structure has been attributed to the intrinsic defects V_O and V_{Zn} [8]; while the blue emission has been associated to a Zn interstitial [26]. The effect of thermal annealing on the NBE intensity of both the O-polar and Zn-polar undoped ZnO samples were also studied. Figure 3(b) shows the relative NBE intensities of the O-polar and Zn-polar ZnO samples against the annealing temperature. The NBE intensities of the samples are normalized against that of the as-grown O-polar sample. As the annealing temperature increases from to 900 ^oC, the relative NBE intensities of the Zn-polar and O-polar samples steadily increase from ~20 to ~120 and from 1 to ~20 respectively.

CL spectroscopy was also used to study the DLE of the undoped O-polar and Zn-polar ZnO samples and the thermal evolution of the DLE upon annealing. Figure 4(a) and (b) respectively show the DLE spectra of the as-grown undoped O-polar and Zn-polar ZnO samples as well as following thermal annealing at 700 ^oC and 900 ^oC. The CL emission was excited with an electron energy of 5 keV, which corresponded to the analysis depth of ~140 nm as determined using CASINO Monte Carlo modelling of the electron energy loss. The DLE emission of the as-grown Zn-face sample is very weak and negligible comparing to its NBE emission (see the PL and CL spectra shown in Figure 3(a) and 6(a), respectively). The peak position and the shape of the DLE line shape depend on both the polarity of the film and annealing temperature. The DLE is contributed from the emissions from more than one defect. The variation in the DLE's peak position and shape is due to change of the relative intensities of the corresponding defect emissions. For the as-grown and 700 ^oC annealed O-

Journal Pre-proof

face ZnO samples, the DLE emission is fitted by two broad components having peaks centered at 1.96 eV (the yellow luminescence, YL) and 2.38 eV (green luminescence, GL1). However, only the GL1 peak was found in the DLE of the O-face ZnO sample after annealing at 900 ^{o}C. For the as-grown Zn-face ZnO sample, the DLE emission also contains two components peaking at 1.81 eV (red luminescence, RL) and 2.54 eV (green luminescence, GL2). It is noteworthy that the GL2 observed in this sample not only differs in peak position to GL1, but also exhibits a different response to H-plasma treatment (to be discussed later). After annealing the Zn-polar sample at 700 ^{o}C, the YL (at 1.99 eV) component is evident and the GL2 found in the as-grown sample changes to GL1 (at 2.41 eV), and after annealing 900 ^{o}C, only GL1 persists.

Depth-resolved CL was used to investigate the in-depth spatial distribution of the DLE's. Figure 5 shows the GL intensities I_{GL} against the electron beam energy between 1-13 keV for the undoped O-polar and Zn-polar ZnO samples annealed at different temperatures. This range of beam energies provided probing depths ranging from ~ 9 to 400 nm, referring to depths corresponding to 70% loss of the electron beam energy. The excitation electron beam power was kept constant for all the measurements by varying the electron beam current. A CL probe depth of 300 nm equal to the film thickness corresponds to the electron beam energy of ~ 11 keV. For O-polar ZnO, the GL1 (2.38 eV) intensity of the as-grown sample is quite uniform all over the film thickness (black open square in the figure 5), as expected for an uniform concentrations of GL1 defects excited by constant power electron beam. After annealing at 700 ^{o}C (red open circles), the overall GL1 depth-resolved intensity drops uniformly by a factor of 0.5 with a more pronounced decrease near the surface. A similar GL1 intensity profile is observed after annealing at 900 ^{o}C (green open triangles), however, conversely there is an increase in the intensity by 3.5 times compared with the as-grown sample. The as grown undoped Zn-polar sample exhibits a mostly uniform

in-depth GL2 profile (solid black squares) that is about 40x weaker than the as-grown O-polar GL1 profile. After heating at 700 ^{o}C (solid red squares) and 900 ^{o}C (solid green squares), the GL2 emission is quenched. The GL1 appears with in-depth profile that is 20x and 700x, respectively more intense than the as grown sample with both profiles showing lower intensities near the surface and towards the bulk, as observed in the annealed O-polarity sample.

Hydrogen plasma treatment study was carried out on the as-grown undoped O-polar and Zn-polar ZnO samples and those annealed at 900 ^{0}C. Figure 6(a) and (b) respectively shows as-grown and 900 ^{o}C annealed undoped O-face ZnO samples before and after the plasma treatment. Figure 6(a) and (b) clearly shows that plasma treatment enhances the near band edge emission (NBE) and quenches the DLE in the O-face samples. The insert of Figure 6(c) shows the CL spectra of the as-grown undoped Zn-polar ZnO sample before and after the plasma treatment. The NBE intensity of the both samples is enhanced by the plasma treatment. Figure 6(c) shows the DLE of the as-grown undoped Zn-polar ZnO samples before and that after the plasma treatment (×50 intensity scale). It was found that the RL and GL2 identified in the as-grown undoped Zn-polar ZnO sample are not removed by the plasma treatment. Figure 6(d) shows the CL spectra of the 900 ^{o}C annealed Zn-polar undoped ZnO sample before and after the plasma treatment, revealing an enhancement of NBE intensity and complete quenching of the GL1. For the O-polar ZnO and Zn-polar ZnO undoped samples annealed at 700 ^{o}C for which GL1 and YL are identified, plasma treatment also removes the two DLE's (CL spectra not shown). To sumarize, the plasma treatment quenches the GL1 and YL and has no effect on the GL2 and RL intensity.

Discussion and Conclusions

Journal Pre-proof

The electron concentration of a semiconductor is dependent on both its shallow donor concentration and its abundance of the compensating defects. In ZnO, H is an important residual shallow donor and widely regarded to be responsible for the n-type conductivity of unintentionally doped ZnO [8, 27, 28]. The electron concentration of the as-grown undoped O-polar ZnO sample is higher than that of the Zn-polar sample by a factor of 3 (6×10^{19} cm^{-3} and 2×10^{19} cm^{-3}, respectively). The as-grown undoped O-polar ZnO sample has a H concentration 3.5 times larger than that of the Zn-polar sample, which is close to the fractional difference of their electron concentration. The higher H concentration in the as-grown undoped O-polar ZnO sample is most likely the cause of its higher electron concentration. For both the O-polar and Zn-polar undoped samples, the H concentration monotonically decrease with increasing annealing temperature. However for the O-polar undoped sample, the electron concentration decreases first when the annealing temperature is $\leq$750 ^{o}C, and then it increases with higher temperature. Following the 750 ^{o}C anneal, the electron concentration drops by 70 % when compared to that of the as-grown value, while the H-concentration drops by the similar amount of 69 %. The drop in the electron concentration with annealing temperature for the O-polar undoped sample with an annealing temperature $\leq$750 ^{o}C is related to the thermal removal of the H.. After annealing at 900 ^{o}C, the H concentration of the O-polar undoped samples slightly decrease but the electron concentration increases from 2×10^{18} cm^{-3} to 4×10^{18} cm^{-3} (i.e. by ~50 %). This implies that observed increase in electron concentration is associated to the reduction in the abundance of compensating defects rather than to an increase in the H shallow donor concentration. The thermal evolution of the electron concentration of the Zn-polar undoped sample decreases monotonically with the annealing temperature, which is not the same as that of the O-polar thermal behavior. After annealing at 900 ^{o}C, the electron concentration of the O-polar undoped sample drops by 95 % compared to its as-grown value, while the H concentration

drops by only 31 %. This implies that the thermal suppression of electron concentration cannot be only due to the thermal removal of H but must be also associated to the thermal creation of compensating defects. It is important to note that annealing at 900 ^{o}C creates and removes compensating defects in Zn-polar and O-polar ZnO undoped samples, respectively.

The results shown in Figure 1(b) reveal that the H concentration in the O-face undoped ZnO sample is higher than that of the undoped Zn-face sample. In our previous study, we have studied the abundance of V_O in the same O-polar and Zn-polar ZnO samples using XPS. The O 1s XPS binding energy spectra were well fitted by three oxygen components, associated with (i) the O^{2-} in the ZnO lattice, (ii) oxygen vacancies and (iii) surface absorbed OH [16]. It was found that the Zn-polar undoped ZnO sample had a slightly stronger relative OH intensity as compared to that of the O-polar sample. This could be due to the favorable bonding of the OH^- to the Zn^{2+} and H^+ to the O^{2-} respectively on the Zn-polar and O-polar surface The NBE PL emission at 10 K peaking at 3.351 eV of the as-grown Zn-polar undoped ZnO has 18x higher intensity than that of the O-polar undoped sample. The 3.351 eV emission line has been associated to the neutral donor bound exciton (D^0X) emission [29]. Additionally, the DLE of the as-grown Zn-polar undoped ZnO sample is negligible as compared to its NBE while that for the O-polar undoped ZnO sample is much stronger. For both the Zn-polar and O-polar ZnO undoped samples, the NBE intensity increases with increasing annealing temperature, however their post heat treatment intensities are different. The relative NBE intensity of the O-polar ZnO sample after annealing at 900 ^{0}C is 20, while that for the Zn-polar sample is 120. The significant higher ultra-violet emission performance of the Zn-polar ZnO material makes it a better choice for luminescence applications as compared to the O-polar ZnO material. The higher NBE intensity and lower DE intensity in the Zn-polar ZnO materials suggests that the Zn-polar material has less defect related non-radiative recombination pathways than the O-polar material.

Journal Pre-proof

The experimental (W,S) data of the O-polar and Zn-polar samples were compared with the theoretical characteristic W-S lines of V_{Zn}, V_{Zn}-V_O, V_O-$2V_{Zn}$, V_{Zn}-$2V_O$ and $4V_{Zn}$. The single type of V_{Zn}-$2V_O$ dominates in the as-grown O-polar ZnO samples while the signals of the others are not detected. For the Zn-polar as-grown sample, co-existence of monovacancy, divacancy and/or trivacancy are found. It is important to point out that vacancy clusters exist in the Zn-polar films and V_{Zn}-$2V_O$ dominates in the O-polar sample although the formation energy of V_{Zn} monovacancy is lower than that of the vacancy clusters [30]. Bang et al. [30] also noted that although the formation energies of the vacancy clusters is high, their dissociation energies are also high. This indicates that once the vacancy clusters were formed it was not easy to be dissociated. Luo et al. [11] commented that the substrate temperature of PLD growth was relatively low temperature at 600 ^oC. V_{Zn} and V_O undergo diffusion during the growth process. With the dissociation energy like 2.5 eV of the divacancy V_{Zn}-V_O given by Bang et al. [30], the corresponding dissociating temperature was estimated to be ~850 ^oC which was higher than the substrate temperature during growth. These arguments strongly suggest that the vacancy cluster once formed from the aggregation of diffusing vacancies is difficult to dissociate thermally. The vacancy cluster formation is thus governed by the kinetics of the vacancy diffusion rather than the formation energy associated with the thermodynamic equilibrium process.

There are two different types of structureless green luminescence observed in the present study, the GL2 (2.54 eV) which is only observed in the as-grown undoped Zn-polar sample with very weak intensity; and the GL1 (2.40 eV) which is observed in all the O-polar undoped samples and the annealed Zn-polar undoped samples. It is found that the H-plasma treatment quenches the GL1 but not the GL2. As H-plasma treatment usually quenches the acceptor type defect, GL1 would be associated with acceptor type defect. Green luminescence without fine structure is usually ascribed to intrinsic vacancy defects in ZnO,

V_O and V_{Zn} [8, 13] and references therein). The intensity of the GL1 is quenched and GL2 is uneffected bythe H-plasma treatment suggesting that these emission peaks are related to V_{Zn} and V_O, respectively. A detailed previous PAS study was performed on the undoped ZnO samples grown by the same PLD system and similar conditions with different oxygen pressures and annealed at different temperatures [11]. It was found that for the O-polar ZnO samples grown with the oxygen pressures from 0 Pa to 1.3 Pa and annealed below at temperatures ≤ 750 ^oC, the V_{Zn}-$2V_O$ complex is the only single type of V_{Zn}-related defect in the sample and no signal from isolated V_{Zn} is detected. As GL1 is found in the CL spectra of the O-polar ZnO sample irrespective of the annealing temperature, the PAS data does not provide the assignment of the GL1 to V_{Zn}.

Annealing the O-polar and Zn-polar undoped ZnO samples has the effect of enhancing the GL1 intensity. The as-grown Zn-polar sample does not exhibit a GL1 emission, however, after annealing at 900 ^oC a GL1 peak is created with an intensity equivalent to that of the O-polar sample after annealing at 900 ^oC. Accordingly, the formation in the GL1 peak in both types of sample after annealing at 900 ^oC is ascribed to the thermal generation of the defect associated with the GL1 peak. Another effect of annealing is the creation of a region of decreasing GL1 intensity in the in-depth profile moving from the bulk towards the surface of the sample (Figure 5). The most likely explanation for this effect is that GL1 defects are created at elevated temperature are sufficiently mobile to diffuse to the surface of the sample where they are annihilated.

In conclusion, undoped O-polar and Zn-polar ZnO films were grown on c-sapphire using PLD. The as-grown O-polar ZnO sample had higher electron concentration than the Zn-polar sample because of its higher H-concentration. The thermal evolution of their electron concentrations were found to be very different. The electron concentration of the Zn-polar undoped ZnO sample monotonically decreases with the annealing temperature,

which was due to the thermal removal of H and thermal creation of compensating defects. For the O-polar undoped ZnO sample, its electron concentration also decreased with annealing temperature $\leq$700 ^{o}C due to the thermal removal of H. However, the electron concentration was observed to increase with annealing temperature >700 ^{o}C, which is attributed to the thermal removal of the compensating defect. The Zn-polar ZnO samples had higher NBE intensity than that of the O-polar sample, which is related to the lower concentrations of defects that act as non-radiative recombination centers. The DLE of the as-grown Zn-polar undoped ZnO sample was negligibly small compared to its NBE, while the as-grown O-polar undoped sample displayed a much more intense DE. Two different GL peaks were observed, centered at 2.38 eV (GL1) and (2.38 eV) and at 2.54 eV (GL2). The GL2, attributed to an oxygen vacancy, was only found in the as-grown undoped Zn-polar ZnO sample while GL1 was observed in the annealed undoped Zn-polar samples as well as all the O-polar undoped ZnO samples. GL1 is probably associated with the acceptor type defect, though its origin still requires further investigation.

ACKNOWLEDGEMENT

This work was financially supported by the Natural Science Foundation of Guangdong Province – General Program (2019A1515012164) and the Research Grant Council, HKSAR (GRF 17302115).

Credit Author Statement

Caiqin Luo: Samples preparation, electrical characterization, photoluminescence study and SIMS characterization

M. Azizar Rahman: CL study

M. R. Phillips: CL study, writing-reviewing and editing the manuscript

C. Ton-That: CL study, writing-reviewing and editing the manuscript

M. Butterling: PAS study

Journal Pre-proof

A. Wagner: PAS study

F. C. C. Ling: Conceptualization, Methodology, writing-reviewing and editing the manuscript

Declaration of interests

☒ The authors declare that they have no known competing financial interests or personal relationships that could have appeared to influence the work reported in this paper.

☐The authors declare the following financial interests/personal relationships which may be considered as potential competing interests:

NA

Journal Pre-proof

References

[1] Ü. Özgür, Y.I. Alivov, C. Liu, A. Teke, M.A. Reshchikov, S. Doğan, V. Avrutin, S.J. Cho, H. Morkoç, A comprehensive review of ZnO materials and devices, Journal of Applied Physics, 98 (2005) 041301.
[2] J.G. Reynolds, C.L. Reynolds, A. Mohanta, J.F. Muth, J.E. Rowe, H.O. Everitt, D.E. Aspnes, Shallow acceptor complexes in p-type ZnO, Applied Physics Letters, 102 (2013) 152114.
[3] L. Liu, J. Xu, D. Wang, M. Jiang, S. Wang, B. Li, Z. Zhang, D. Zhao, C.X. Shan, B. Yao, D.Z. Shen, p-Type conductivity in N-doped ZnO: the role of the N(Zn)-V(O) complex, Phys Rev Lett, 108 (2012) 215501.
[4] S. Limpijumnong, S.B. Zhang, S.H. Wei, C.H. Park, Doping by large-size-mismatched impurities: the microscopic origin of arsenic- or antimony-doped p-type zinc oxide, Phys Rev Lett, 92 (2004) 155504.
[5] Y.F. Hsu, Y.Y. Xi, K.H. Tam, A.B. Djurisic, J.M. Luo, C.C. Ling, C.K. Cheung, A.M.C. Ng, W.K. Chan, X. Deng, C.D. Beling, S. Fung, K.W. Cheah, P.W.K. Fong, C.C. Surya, Undoped p-type ZnO nanorods synthesized by a hydrothermal method, Advanced Functional Materials, 18 (2008) 1020-1030.
[6] K.M. Johansen, L. Vines, T.S. Bjørheim, R. Schifano, B.G. Svensson, Aluminum Migration and Intrinsic Defect Interaction in Single-Crystal Zinc Oxide, Physical Review Applied, 3 (2015) 024003.
[7] D.C. Look, K.D. Leedy, L. Vines, B.G. Svensson, A. Zubiaga, F. Tuomisto, D.R. Doutt, L.J. Brillson, Self-compensation in semiconductors: The Zn vacancy in Ga-doped ZnO, Physical Review B, 84 (2011) 115202.
[8] M.D. McCluskey, S.J. Jokela, Defects in ZnO, Journal of Applied Physics, 106 (2009) 071101.
[9] A. Janotti, C.G. Van de Walle, Native point defects in ZnO, Physical Review B, 76 (2007) 165202.
[10] F. Tuomisto, V. Ranki, K. Saarinen, D.C. Look, Evidence of the Zn vacancy acting as the dominant acceptor in n-type ZnO, Phys Rev Lett, 91 (2003) 205502.
[11] Z. Wang, C. Luo, W. Anwand, A. Wagner, M. Butterling, M.A. Rahman, M.R. Phillips, C. Ton-That, M. Younas, S. Su, F.C. Ling, Vacancy cluster in ZnO films grown by pulsed laser deposition, Scientific reports, 9 (2019) 3534.
[12] S. Lany, A. Zunger, Dopability, intrinsic conductivity, and nonstoichiometry of transparent conducting oxides, Phys Rev Lett, 98 (2007) 045501.

[13] C. Ton-That, L. Weston, M.R. Phillips, Characteristics of point defects in the green luminescence from Zn- and O-rich ZnO, Physical Review B, 86 (2012) 115205.
[14] Y.K. Frodason, K.M. Johansen, T.S. Bjørheim, B.G. Svensson, A. Alkauskas, Zn vacancy as a polaronic hole trap in ZnO, Physical Review B, 95 (2017) 094105.
[15] V.C. Jesús Zúñiga-Pérez, Liverios Lymperakis, Xiang Kong, Achim Trampert, Sergio FernándezGarrido, Oliver Brandt, Hubert Renevier, Stacia Keller, Karine Hestroffer, Markus R. Wagner, Juan Sebastián Reparaz, Fatih Akyol, Siddharth Rajan, Stéphanie Rennesson, Tomás Palacios, and Guy Feuillet, Polarity in GaN and ZnO: Theory, measurement, growth, and devices, Applied Physics Reviews, 3 (2016) 041303.
[16] C.-Q. Luo, F.C.-C. Ling, M.A. Rahman, M. Phillips, C. Ton-That, C. Liao, K. Shih, J. Lin, H.W. Tam, A.B. Djurišić, S.-P. Wang, Surface polarity control in ZnO films deposited by pulsed laser deposition, Applied Surface Science, 483 (2019) 1129-1135.
[17] E.M. Kaidashev, M. Lorenz, H. von Wenckstern, A. Rahm, H.C. Semmelhack, K.H. Han, G. Benndorf, C. Bundesmann, H. Hochmuth, M. Grundmann, High electron mobility of epitaxial ZnO thin films on c-plane sapphire grown by multistep pulsed-laser deposition, Applied Physics Letters, 82 (2003) 3901-3903.
[18] S.I. BJ Jin, SY Lee, Violet and UV luminescence emitted from ZnO thin films grown on sapphire by pulsed laser deposition, Thin Solid Films, 366 (2000) 107.
[19] X.Q. Wei, B.Y. Man, M. Liu, C.S. Xue, H.Z. Zhuang, C. Yang, Blue luminescent centers and microstructural evaluation by XPS and Raman in ZnO thin films annealed in vacuum, N2 and O2, Physica B: Condensed Matter, 388 (2007) 145-152.
[20] S.Z. Y.R. Ryu, D.C. Look, J.M. Wrobel, H.M. Jeong, H.W. White, Synthesis of p-type ZnO"lms, Journal of Crystal Growth, 216 (2000) 330.
[21] H. Tampo, P. Fons, A. Yamada, K.K. Kim, H. Shibata, K. Matsubara, S. Niki, H. Yoshikawa, H. Kanie, Determination of crystallographic polarity of ZnO layers, Applied Physics Letters, 87 (2005) 141904.
[22] X. Wang, Y. Tomita, O.-H. Roh, M. Ohsugi, S.-B. Che, Y. Ishitani, A. Yoshikawa, Polarity control of ZnO films grown on nitrided c-sapphire by molecular-beam epitaxy, Applied Physics Letters, 86 (2005) 011921.
[23] S.-C. Han, J.-K. Kim, J.Y. Kim, K.-K. Kim, H. Tampo, S. Niki, J.-M. Lee, Formation of Hexagonal Pyramids and Pits on V-/VI-Polar and III-/II-Polar GaN/ZnO Surfaces by Wet Etching, Journal of The Electrochemical Society, 157 (2010) D60.
[24] F. Tuomisto, I. Makkonen, Defect identification in semiconductors with positron annihilation: Experiment and theory, Reviews of Modern Physics, 85 (2013) 1583-1631.
[25] I. Makkonen, E. Korhonen, V. Prozheeva, F. Tuomisto, Identification of vacancy defect complexes in transparent semiconducting oxides ZnO, In2O3 and SnO2, J. Phys. Condens. Matter, 28 (2016) 224002.
[26] H. Zeng, G. Duan, Y. Li, S. Yang, X. Xu, W. Cai, Blue Luminescence of ZnO Nanoparticles Based on Non-Equilibrium Processes: Defect Origins and Emission Controls, Advanced Functional Materials, 20 (2010) 561-572.
[27] S.F. Cox, E.A. Davis, S.P. Cottrell, P.J. King, J.S. Lord, J.M. Gil, H.V. Alberto, R.C. Vilao, J. Piroto Duarte, N. Ayres de Campos, A. Weidinger, R.L. Lichti, S.J. Irvine, Experimental confirmation of the predicted shallow donor hydrogen state in zinc oxide, Phys Rev Lett, 86 (2001) 2601-2604.
[28] C.G.V.d. Walle, Hydrogen as a Cause of Doping in Znic Oxide, Physical Review Letters, 85 (2000) 1012.
[29] B.K. Meyer, H. Alves, D.M. Hofmann, W. Kriegseis, D. Forster, F. Bertram, J. Christen, A. Hoffmann, M. Straßburg, M. Dworzak, U. Haboeck, A.V. Rodina, Bound exciton and donor–acceptor pair recombinations in ZnO, physica status solidi (b), 241 (2004) 231-260.
[30] J. Bang, Y.-S. Kim, C.H. Park, F. Gao, S.B. Zhang, Understanding the presence of vacancy clusters in ZnO from a kinetic perspective, Applied Physics Letters, 104 (2014) 252101.

Journal Pre-proof

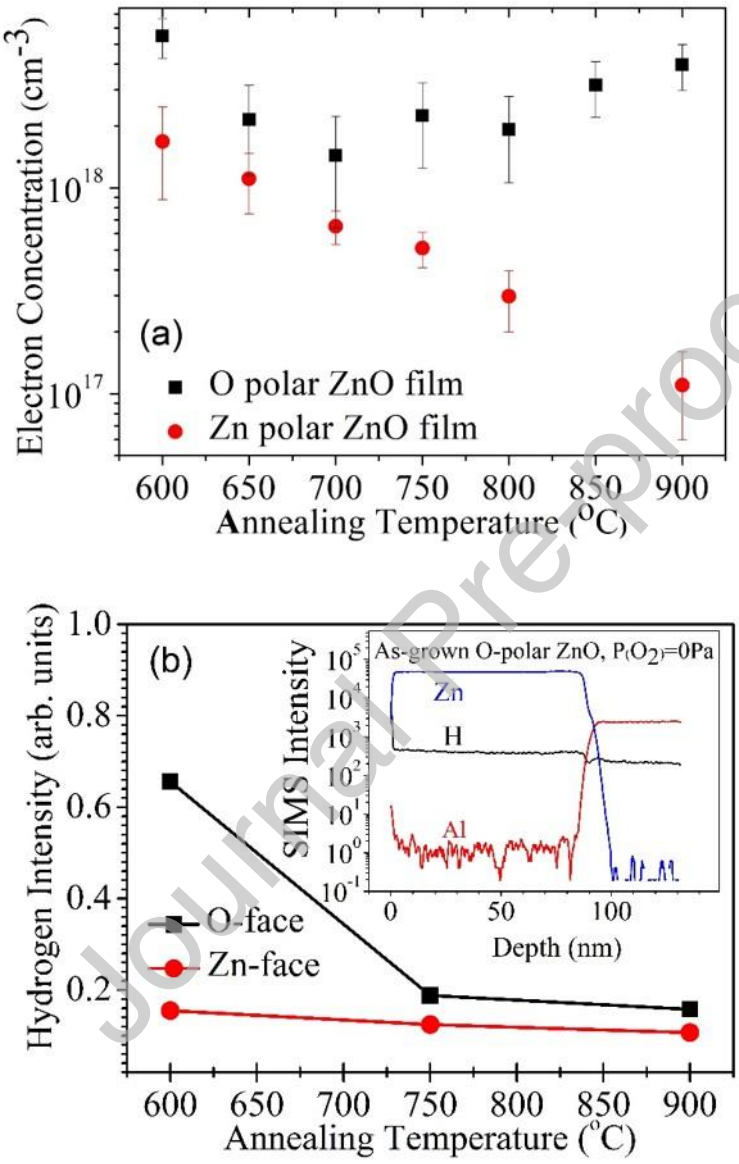

Figure 1 (a) shows the electron concentration versus annealing temperature for the O-polar and Zn-polar ZnO samples. The relative H intensity against the annealing temperature for the O-face and Zn-face ZnO samples is presented in Figure 1(b). The data of annealing temperature equal to 600 ^{o}C are those for the as-grown samples grown at 600 ^{o}C. The insert of 1 (b) shows the SIMS depth profile of H, Zn and Al for the as-grown O-polar ZnO sample.

Journal Pre-proof

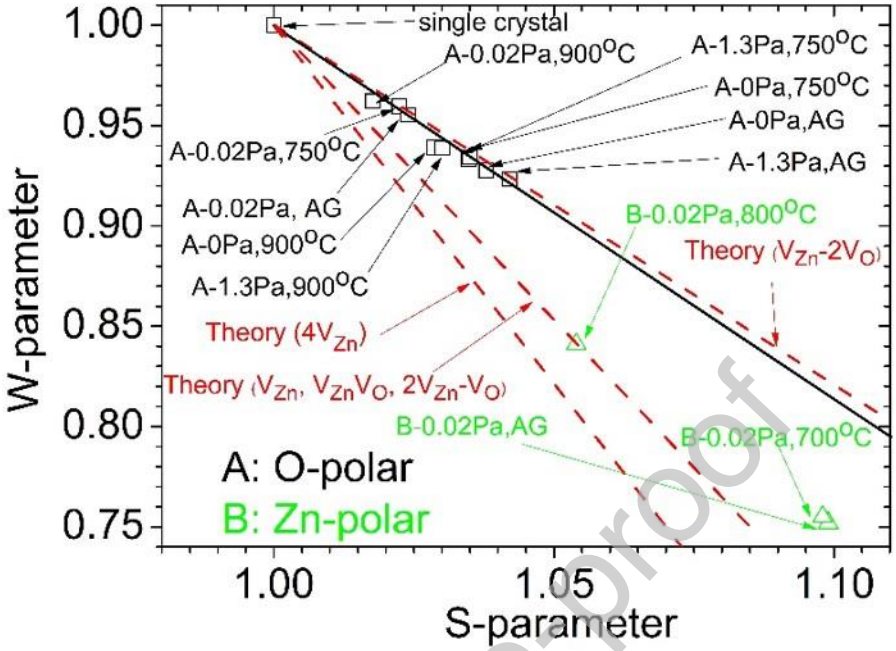

Figure 2 shows the W-S parameter plot for the CDBS study of the O-polar and Zn-polar samples. The black square symbols refer to the (W,S) data of the O-polar ZnO sample grown with different $P(O_2)$=0 Pa to 1.3 Pa annealed at different temperatures are reproduced from Luo et al. [16]. These data with annealing temperature ≤750 °C lay on the theoretical characteristic W-S line of V_{Zn}-$2V_O$. The red dotted lines refer to the theoretical W-S lines of the different V_{Zn} and vacancy clusters [11]. It is significant to note that the V_{Zn}, $V_{Zn}V_O$ and $2V_{Zn}$-V_O have characteristic W-S lines that are indistinguishable. The green triangle symbols are the (W,S) data of the Zn-polar ZnO sample grown with $P(O_2)$=0 Pa and annealed at different temperatures.

Journal Pre-proof

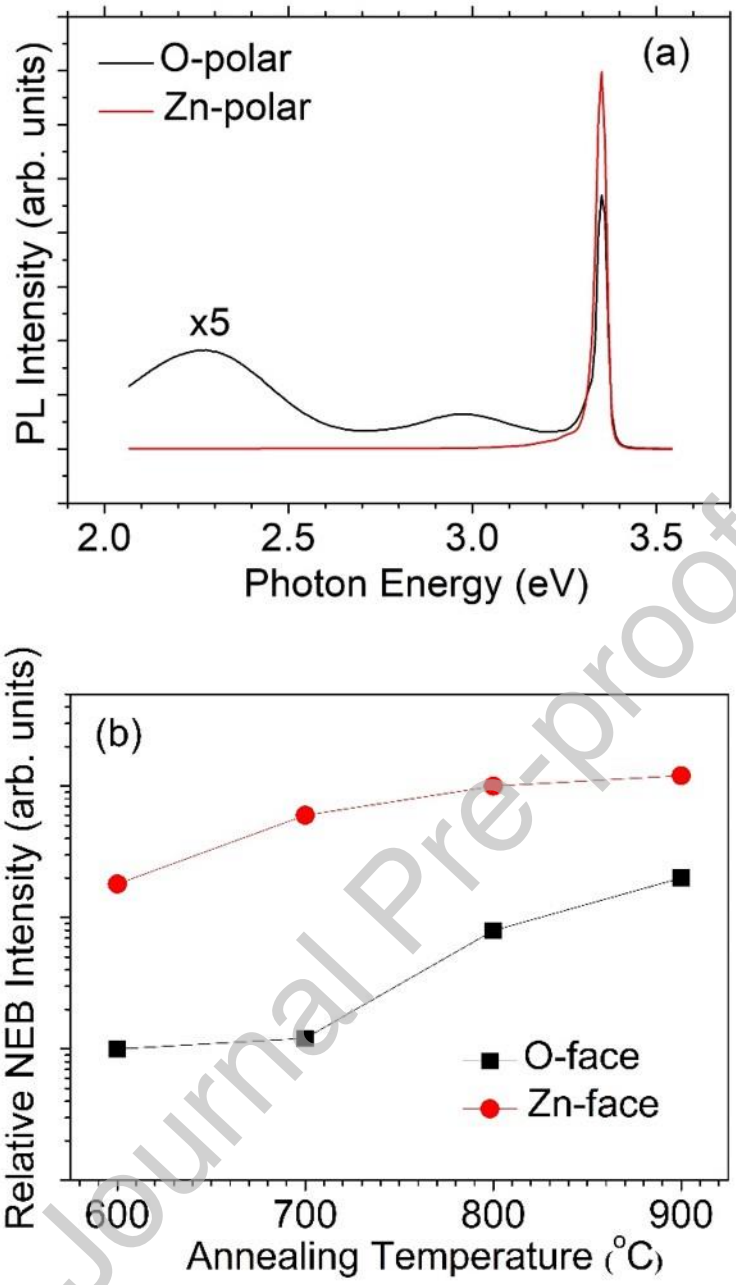

Journal Pre-proof

Figure 3 (a) The low temperature (10 K) PL spectra of the as-grown O-polar and Zn-polar ZnO samples; and (b) The relative NBE intensities of the PL spectra for the as-grown O-polar and Zn-polar ZnO samples. The relative NBE intensity is normalized against the NBE intensity of the as-grown O-polar sample. The data of annealing temperature equal to 600 ^{o}C are those for the as-grown samples grown at 600 ^{o}C.

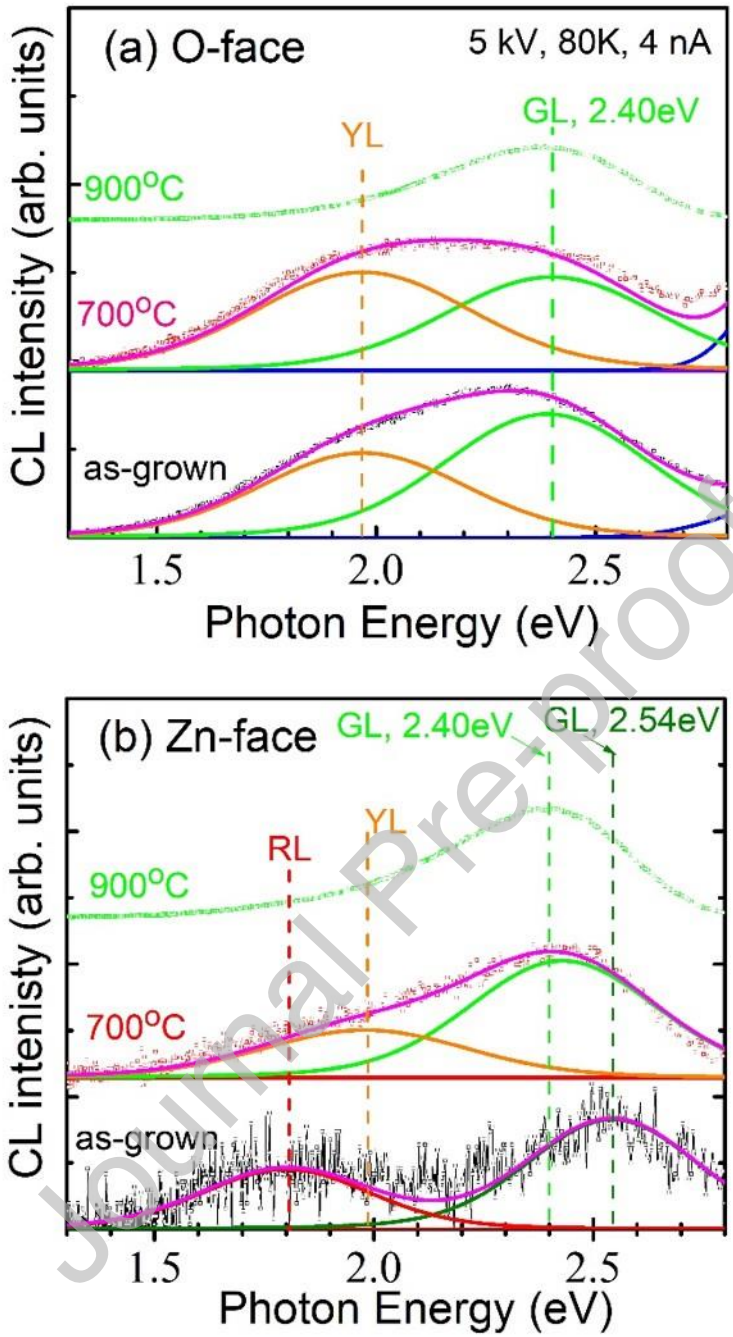

Figure 4 (a) and (b) respectively show the DLE CL spectra for the O-polar and Zn-polar ZnO samples annealed at different temperatures. The DLEs of the as-grown and 700 ^{o}C annealed ZnO samples are well fitted by the superposition two-Gaussian and those for the 900 ^{o}C annealed samples are well fitted by the single Gaussian component. The lines represent the fitted Gaussian peaks.

Journal Pre-proof

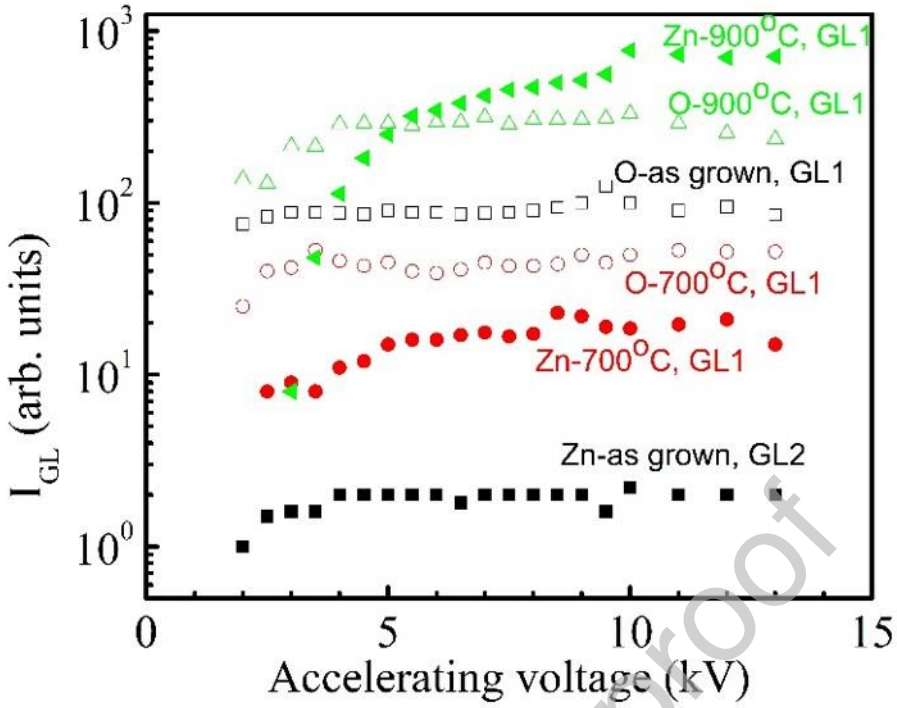

Figure 5 shows the depth-resolved CL results. The intensities of the GL1 and GL2 as plotted versus the electron beam energy at constant power for the O-polar and Zn-polar ZnO samples annealed at different temperatures.

Journal Pre-proof

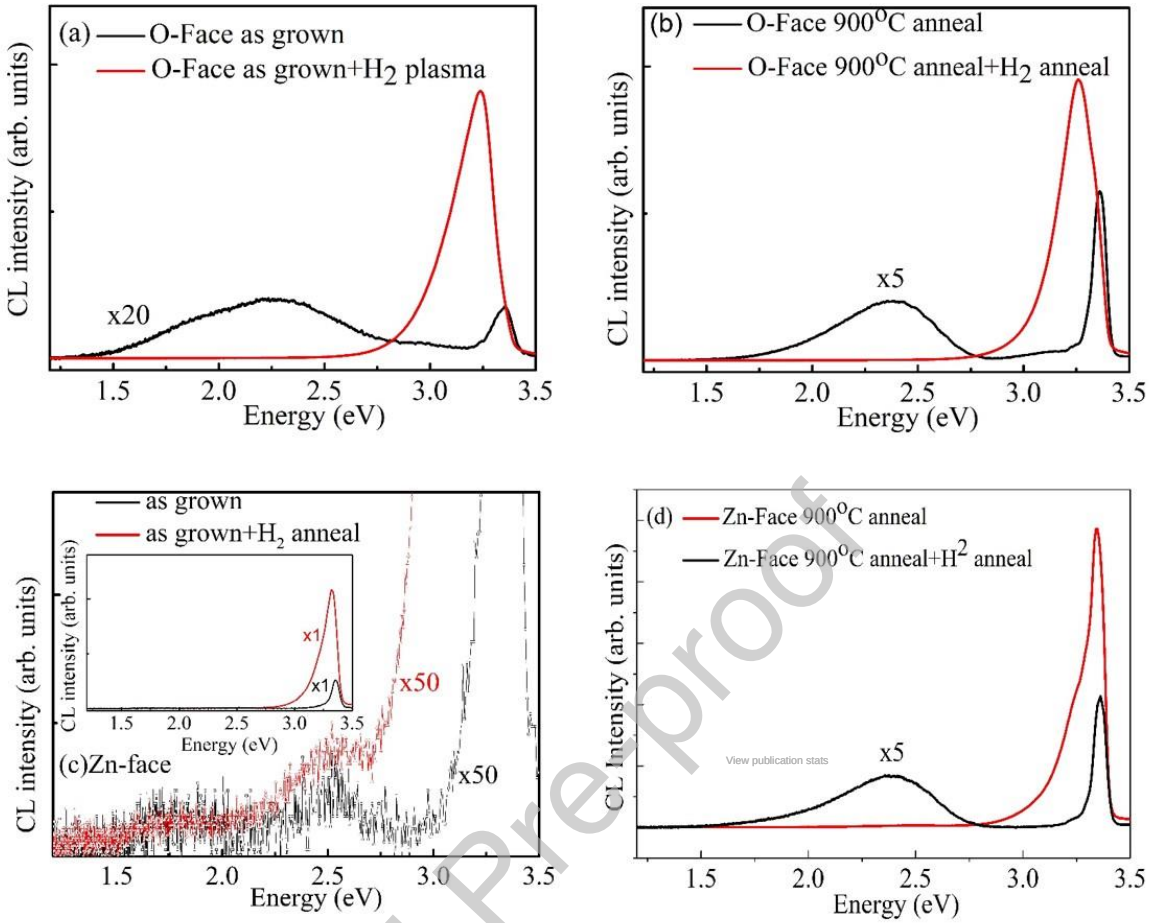

Figure 6 (a) and (b) are respectively the CL spectra of the as-grown and 900 °C annealed O-polar ZnO samples before and after the H plasma treatment. Fig 6(c) is the ×50 y-scale DLE of the as-grown Zn-polar sample before and after the H plasma treatment. The insert of (c) and (d) are those of the as-grown and 900 °C annealed O-polar and Zn-polar samples before and after the H plasma treatment. The insert in Fig 6 (c) and Fig 6 (d) show the CL spectra from the as-grown and 900 °C annealed O-polar and Zn-polar samples before and after the H plasma treatment, respectively.

Journal Pre-proof